

## **k·p theory of energy bands, wave functions, and optical selection rules in strained tetrahedral semiconductors**

P. Enders, A. Bärwolff, and M. Woerner

*Max-Born-Institut für Nichtlineare Optik und Kurzzeitspektroskopie, Rudower Chausse 6, D-12489 Berlin, Germany*

D. Suisky

*Institut für Physik, Humboldt-Universität zu Berlin, Invalidenstrasse 110, D-10115 Berlin, Germany*

(Received 14 February 1995)

This paper examines an eight-band  $\mathbf{k}\cdot\mathbf{p}$  theory of strained semiconductors yielding energy bands, wave functions, and momentum matrices. Only if the symmetry of the strained crystal is accounted for in *all* terms of the Hamiltonian, a consistent definition and calculation of the momentum matrix becomes possible. The band structure and wave functions are nonanalytical functions of strain and crystal momentum. For strained crystals, the extrapolation from the  $\Gamma$  point into the Brillouin zone, such as the effective-mass approximation for the optical-matrix elements, can be misleading. For certain cases, the heavy- and light-hole isoenergetic surfaces form complex figures resembling the indicatrix of birefringent biaxial crystals. The symmetry of the hole wave functions causes dichroism for photon energies close to the gap energy, while the crystal becomes optically isotropic for larger photon energies. Numerical results are presented for the eight-band  $\mathbf{k}\cdot\mathbf{p}$  model of biaxially strained bulklike  $1.3\text{-}\mu\text{m-In}_x\text{Ga}_{1-x}\text{As}_y\text{P}_{1-y}$  on InP being an important material in optoelectronics.

### I. INTRODUCTION

Strained tetrahedral semiconductors are superior to unstrained materials with respect to various properties and novel effects.<sup>1</sup> For this, they are subject to intensive and comprehensive investigation. For theoretically modeling the band structure near the band edges, the  $\mathbf{k}\cdot\mathbf{p}$  method<sup>1,2</sup> is the favorite tool. Calculating the electronic properties of direct band-gap semiconductors around the  $\Gamma$  point, at least an eight-band model is required, that comprises conduction band (C), heavy holes (HH), light holes (LH), and spin-orbit interaction split-off band (SO) plus spin. A comprehensive derivation of the corresponding Hamiltonian matrix elements has been given by Trebin, Rössler, and Ranvaud.<sup>3</sup> Using group-theoretical methods, they extended the work by Bir and Pikus<sup>4</sup> and included an external quantizing magnetic field, in order to extract the empirical  $\mathbf{k}\cdot\mathbf{p}$  model parameters from quantum resonances in the valence bands of  $p$ -type InSb. The group-theoretical approach has the advantage of more systematically accounting for symmetry, what facilitates the determination of independent model parameters, and the classification of the system's behavior, e.g., optical transitions. Bahder<sup>5</sup> has derived various terms by explicitly performing the Pikus-Bir<sup>4,6</sup> transformation, with detailed treatment of the spin-orbit interaction terms. This approach is more obvious and will be adopted here.

All papers we are aware of account for the strain strictly up to first order. Being consistent within the order of approximation, this has, nevertheless, two disadvantages. First, it violates the von Neumann principle, that the physical observables of a system exhibit the same symmetry as this system.<sup>7</sup> This is our main objective against

such a treatment. Second, the momentum operator,  $\mathbf{p}_{\mathbf{k}\cdot\mathbf{p}} = (m/\hbar)\partial\mathbf{H}_{\mathbf{k}\cdot\mathbf{p}}/\partial\mathbf{k}$ , becomes inconsistent, when the matrix elements of the Hamiltonian  $\mathbf{H}_{\mathbf{k}\cdot\mathbf{p}}$  are treated nonuniformly. Furthermore, Kane's<sup>8</sup> rotation of the  $z$  axis on the  $k$  axis becomes useless. The goal of this paper is to show that these shortcomings are removed immediately after applying the Pikus-Bir transformation to the terms of second order in  $k$  also.

Often, it is said that a TE electromagnetic field (the electrical field vector  $\mathbf{E}||xy$  plane) is (predominantly) absorbed or amplified by the heavy holes, while a TM field ( $\mathbf{E}||z$ ) is absorbed or amplified by the light holes. This holds true at the  $\Gamma$  point, if the  $z$  axis is the axis of quantization. However, the corresponding electron-hole transitions take place not at the  $\Gamma$  point, since here the density of states vanishes, but involve states with  $k > 0$ . Nonhydrostatic stress lifts the degeneracy of the HH and LH band edges ( $\Gamma_8$  states) and can cause an HH-LH band mixing and anticrossing of the  $\Gamma$  point ( $k > 0$ ; cf, e.g., Chuang<sup>9</sup>). This means a significant change of the symmetry of the HH and LH wave functions, which is important for the efficiency of various scattering processes or for the interaction with electromagnetic waves. In fact, the band energies are *not analytical* functions of strain and crystal momentum.<sup>10-12</sup> Calculating the wave functions and the momentum matrix elements as functions of crystal momentum and stress, the symmetry changes of the wave functions will be shown to be the clue to the understanding of the irregular behavior of the momentum matrix and, thus, oscillator strengths in such materials. In particular, the selection rules are strongly modified for optical transitions near the  $\Gamma$  point.

Thus, this paper is organized as follows. In Sec. II, we first write down the  $8\times 8$   $\mathbf{k}\cdot\mathbf{p}$  Hamilton matrix with

strain on the base of the Pikus-Bir transformation. All terms used later for numerical computations are explicitly given, in order to facilitate comparison with other approaches and the derivation of the momentum matrix. Some remarks on Kane's rotation of the coordinate system follow. Then, a consistent definition of the momentum matrix will be given which continues to obey the  $f$  sum rule and the exact relation<sup>13</sup>  $\langle \nu \mathbf{k} | \mathbf{p} | \nu \mathbf{k} \rangle = (m/\hbar) \partial E_{\nu \mathbf{k}} / \partial \mathbf{k}$  under strain. These results are compared with other approaches. In Sec. III, their quantitative consequences are illustrated through computations for biaxially strained bulklike  $1.3\text{-}\mu\text{m-In}_x\text{Ga}_{1-x}\text{As}_y\text{P}_{1-y}$  on InP. This is an interesting material for optoelectronics, but so far its band structure has not been greatly investigated by means of an eight-band model. First, the energy bands are considered. For certain parameter values, the HH and LH isoenergy surfaces form figures resembling the indicatrix of birefringent biaxial crystals.<sup>14</sup> The character of the band states is investigated by means of the symmetry of the wave functions. The numerical examination of the effective-mass approximations for the oscillator strength will demonstrate that extrapolations from the  $\Gamma$  point to the Brillouin zone  $k > 0$  are not generally allowed. Section IV summarizes the results. The Appendix sketches the calculation of the oscillator strengths by means of a projection operator method, which circumvents the computation of the eigenfunctions of the  $\mathbf{k}\cdot\mathbf{p}$  Hamiltonian.

## II. $\mathbf{k}\cdot\mathbf{p}$ THEORY WITH STRAIN

### A. Hamilton matrix

A homogeneous strain is a singular perturbation. This singularity can be removed by means of the Pikus-Bir

transformation, i.e., the transformation of the coordinate system of the strained crystal  $\{\mathbf{x}_\varepsilon\}$  to that of the unstrained one  $\{\mathbf{x}\}$ :  $\mathbf{x}_\varepsilon = (1 + \varepsilon) \cdot \mathbf{x}$ , where  $\varepsilon$  is the strain tensor. Correspondingly, the crystal momentum is transformed as  $\mathbf{k}_\varepsilon = (1 - \varepsilon) \cdot \mathbf{k}$ . Most results of the  $\mathbf{k}\cdot\mathbf{p}$  theory can be carried over from the unstrained to the strained case just by replacing the crystal momentum component  $k_\alpha$  with  $(\delta_{\alpha\alpha'} - \varepsilon_{\alpha\alpha'})k_{\alpha'}$  ( $\alpha, \alpha' = x, y, z$ ; summation over repeated indices) and adding the deformation potential contribution. In particular, the Hamiltonian of the strained system,  $\mathbf{H}_\varepsilon(\mathbf{k}, \varepsilon)$ , can be obtained from the Hamiltonian without strain,  $\mathbf{H}_0(\mathbf{k})$ , as

$$\mathbf{H}_\varepsilon(\mathbf{k}, \varepsilon) = \mathbf{H}_0[(1 - \varepsilon) \cdot \mathbf{k}] + \mathbf{D}(\varepsilon), \quad (1)$$

where  $\mathbf{D}(\varepsilon)$  denotes the deformation potential contribution (cf. Ref. 5). It can be taken apart into

$$\begin{aligned} \mathbf{H}_\varepsilon(\mathbf{k}, \varepsilon) = & \mathbf{H}_0 + \mathbf{H}_\Delta + \mathbf{D}(\varepsilon) + \mathbf{H}_1(\mathbf{k}_\varepsilon) \\ & + \mathbf{H}_2(\mathbf{k}_\varepsilon), \quad \mathbf{k}_\varepsilon \equiv (1 - \varepsilon) \cdot \mathbf{k}, \end{aligned} \quad (2)$$

where  $\mathbf{H}_0$  represents the energies of the basis states,  $\mathbf{H}_\Delta$  the spin-orbit interaction,  $\mathbf{D}(\varepsilon)$  the deformation potential interaction, and  $\mathbf{H}_1(\mathbf{k}_\varepsilon)$  and  $\mathbf{H}_2(\mathbf{k}_\varepsilon)$  the  $\mathbf{k}\cdot\mathbf{p}$  interaction of first and second order, respectively. Within the basis of atomiclike states (the superscript  $T$  denotes the transpose)

$$\mathbf{u}_{\text{at}} = (S\uparrow, X\uparrow, Y\uparrow, Z\uparrow, S\downarrow, X\downarrow, Y\downarrow, Z\downarrow)^T \quad (\mathbf{k}_0 = 0) \quad (3)$$

of the eight-band model for the cubic, unstrained material, the dominant contributions are represented through the following matrices (cf. Refs. 3 and 6):

$$\mathbf{H}_0 = \begin{pmatrix} E_g & 0 & 0 & 0 & 0 & 0 & 0 & 0 \\ 0 & -\frac{\Delta}{3} & 0 & 0 & 0 & 0 & 0 & 0 \\ 0 & 0 & -\frac{\Delta}{3} & 0 & 0 & 0 & 0 & 0 \\ 0 & 0 & 0 & -\frac{\Delta}{3} & 0 & 0 & 0 & 0 \\ 0 & 0 & 0 & 0 & E_g & 0 & 0 & 0 \\ 0 & 0 & 0 & 0 & 0 & -\frac{\Delta}{3} & 0 & 0 \\ 0 & 0 & 0 & 0 & 0 & 0 & -\frac{\Delta}{3} & 0 \\ 0 & 0 & 0 & 0 & 0 & 0 & 0 & -\frac{\Delta}{3} \end{pmatrix}. \quad (4a)$$

$E_g$  is the fundamental gap of the unstrained material and  $\Delta$  the spin-orbit interaction energy there. The upper valence-band edge ( $\Gamma_8$  states) lies at the energy  $E = 0$ , when including the  $\mathbf{k}$ -independent spin-orbit interaction

$$\mathbf{H}_\Delta = \frac{\Delta}{3} \begin{bmatrix} 0 & 0 & 0 & 0 & 0 & 0 & 0 & 0 \\ 0 & 0 & -i & 0 & 0 & 0 & 0 & 1 \\ 0 & i & 0 & 0 & 0 & 0 & 0 & -i \\ 0 & 0 & 0 & 0 & 0 & -1 & i & 0 \\ 0 & 0 & 0 & 0 & 0 & 0 & 0 & 0 \\ 0 & 0 & 0 & -1 & 0 & 0 & i & 0 \\ 0 & 0 & 0 & -i & 0 & -i & 0 & 0 \\ 0 & 1 & i & 0 & 0 & 0 & 0 & 0 \end{bmatrix}. \quad (4b)$$

The Hamilton matrix of the deformation potential interaction reads

$$\mathbf{D}(\epsilon) = \begin{bmatrix} a_s(\epsilon_{xx} + \epsilon_{yy} + \epsilon_{zz}) & 0 & 0 & 0 \\ 0 & \mathbf{D3}(\epsilon) & 0 & 0 \\ 0 & 0 & a_s(\epsilon_{xx} + \epsilon_{yy} + \epsilon_{zz}) & 0 \\ 0 & 0 & 0 & \mathbf{D3}(\epsilon) \end{bmatrix}, \quad (4c)$$

with

$$\mathbf{D3}(\epsilon) = \begin{bmatrix} l_\epsilon \epsilon_{xx} + m_\epsilon(\epsilon_{yy} + \epsilon_{zz}) & n_\epsilon \epsilon_{xy} & n_\epsilon \epsilon_{xz} \\ n_\epsilon \epsilon_{yx} & l_\epsilon \epsilon_{yy} + m_\epsilon(\epsilon_{xx} + \epsilon_{zz}) & n_\epsilon \epsilon_{yz} \\ n_\epsilon \epsilon_{zx} & n_\epsilon \epsilon_{zy} & l_\epsilon \epsilon_{zz} + m_\epsilon(\epsilon_{yy} + \epsilon_{xx}) \end{bmatrix}, \quad (4c')$$

where  $a_s$ ,  $l_\epsilon$ ,  $m_\epsilon$ , and  $n_\epsilon$  are deformation potentials.  $\mathbf{D3}(\epsilon)$  exhibits the same symmetry as the Shockley matrix  $\mathbf{S}$  given below.

We neglect the first-order  $\mathbf{k}\cdot\mathbf{p}$  coupling between the  $p$ -like basis states and the second-order  $\mathbf{k}\cdot\mathbf{p}$  coupling between the  $s$ - and the  $p$ -like basis states, since they are believed to be small.<sup>3</sup> The form of these coupling terms is given in Ref. 4. Then,

$$\mathbf{H}_1(\mathbf{k}_\epsilon) = \begin{bmatrix} \mathbf{H4}(\mathbf{k}_\epsilon) & 0 \\ 0 & \mathbf{H4}_1(\mathbf{k}_\epsilon) \end{bmatrix}, \quad (4d)$$

with

$$\mathbf{H4}_1(\mathbf{k}_\epsilon) = \begin{bmatrix} 0 & iPk_{x\epsilon} & iPk_{y\epsilon} & iPk_{z\epsilon} \\ -iPk_{x\epsilon} & 0 & 0 & 0 \\ -iPk_{y\epsilon} & 0 & 0 & 0 \\ -iPk_{z\epsilon} & 0 & 0 & 0 \end{bmatrix}, \quad k_{a\epsilon} \equiv k_a - \sum_{\beta=x}^z \epsilon_{a\beta} k_\beta, \quad (4d')$$

where  $P$  is essentially the real-valued momentum matrix element  $\langle S\uparrow | \partial_x | X\uparrow \rangle$ . The free-electron and second-order  $\mathbf{k}\cdot\mathbf{p}$  interaction contributions are contained in the matrix

$$\mathbf{H}_2(\mathbf{k}_\epsilon) = \begin{bmatrix} Ak_\epsilon^2 & 0 & 0 & 0 \\ 0 & \mathbf{S}(\mathbf{k}_\epsilon) & 0 & 0 \\ 0 & 0 & Ak_\epsilon^2 & 0 \\ 0 & 0 & 0 & \mathbf{S}(\mathbf{k}_\epsilon) \end{bmatrix} \quad \text{with } k_\epsilon^2 = k_{x\epsilon}^2 + k_{y\epsilon}^2 + k_{z\epsilon}^2, \quad (4e)$$

$$\mathbf{S}(\mathbf{k}_\epsilon) = \begin{bmatrix} Lk_{x\epsilon}^2 + M(k_{y\epsilon}^2 + k_{z\epsilon}^2) & Nk_{x\epsilon}k_{y\epsilon} & Nk_{x\epsilon}k_{z\epsilon} \\ Nk_{y\epsilon}k_{x\epsilon} & Lk_{y\epsilon}^2 + M(k_{z\epsilon}^2 + k_{x\epsilon}^2) & Nk_{y\epsilon}k_{z\epsilon} \\ Nk_{z\epsilon}k_{x\epsilon} & Nk_{z\epsilon}k_{y\epsilon} & Lk_{z\epsilon}^2 + M(k_{x\epsilon}^2 + k_{y\epsilon}^2) \end{bmatrix}. \quad (4e')$$

$\mathbf{S}(\mathbf{k}_\epsilon)$  is the Shockley matrix<sup>15</sup> modified through the strain transformation of the reciprocal space coordinate system. This modification can be derived by noting that the parameters  $L$ ,  $M$ , and  $N$  contain the free-electron term,  $\hbar^2 k^2/2m$ , and momentum matrix elements with the

remote states,  $R$ , e.g.,

$$L = \frac{\hbar^2}{2m} + \frac{\hbar^2}{m^2} \sum_{R \neq S, X, Y, Z} \frac{\langle X\uparrow | p_x | R\uparrow \rangle \langle R\uparrow | p_x | X\uparrow \rangle}{E_X - E_R}. \quad (5)$$

Then, the transformation of the momentum operator in the strained crystal,  $\mathbf{p}_\varepsilon = (1 - \varepsilon) \cdot \mathbf{p} + O(\varepsilon^2)$ , is carried over onto the quasimomentum  $\mathbf{k}$  of the unstrained crystal [cf. Ref. 5, Eq. (29.14)]. Remember that the functions  $R$  belong to the unstrained crystal and, thus, are strain independent. Analogously, the term  $Ak^2$  is treated.

The explicit formulas (4) show that the total Hamiltonian (2) exhibits the symmetry of the strained crystal only, if *all*  $\mathbf{k} \cdot \mathbf{p}$  terms are transformed in the *same* way. Some practical consequences of this point of view are examined in the following subsections.

#### B. Kane's rotation of the coordinate system on the $\mathbf{k}$ axis in the case with strain

For  $\mathbf{k} \parallel \mathbf{z}$ ,  $\mathbf{z}$  being the unit vector in the [001] direction, the representation (4) of the Hamiltonian (2) is particularly simple; for shear-free strain ( $\varepsilon_{xy} = \varepsilon_{xz} = \varepsilon_{yz} = 0$ ), it even diagonalizes into two  $4 \times 4$  blocks and the HH band separates. For this, Kane<sup>8</sup> has introduced a  $\mathbf{k}$ -dependent rotation of the coordinate system (without strain) such that the  $\mathbf{z}$  axis of the new coordinate system,  $\mathbf{z}'$ , is always parallel to the  $\mathbf{k}$  vector. Obviously, this idea applies to the Hamiltonian with strain only, if *all*  $k_\alpha$ 's are replaced with  $(k_\alpha - \varepsilon_{\alpha\beta} k_\beta)$ . Of course, this replacement has to be done in the transformation matrices as well.

This transformation works well for all parts of the matrices (4), which are cubic-isotropic. For the Shockley matrix (4e), this would mean  $\mathbf{S}_{\alpha\beta} = c_1 \mathbf{k}_\varepsilon^2 \delta_{\alpha\beta} + c_2 k_{\varepsilon\alpha} k_{\varepsilon\beta}$ , where  $c_{1,2}$  are  $\mathbf{k}$  independent. This is the case for  $LN \equiv L - M - N = 0$ .  $LN = 0$  is never met, however, in

contrast,  $LN \neq 0$  is responsible for the characteristic warping of the valence bands. Fortunately, the terms which prevent the  $4 \times 4$  block diagonalization of  $\mathbf{H}_2$  are small and can be neglected in most cases.<sup>16</sup> More difficulties are caused by certain non-negligible off-diagonal matrix elements generated by the transformation of  $\mathbf{D3}(\varepsilon)$ . Here, further work is necessary.

#### C. Consistent definition of the momentum operator

Within the  $\mathbf{k} \cdot \mathbf{p}$  representation of the Hamiltonian,  $\mathbf{H}_{\mathbf{k} \cdot \mathbf{p}}$ , without strain, the momentum matrix reads (Ref. 5, Sec. 36)

$$\langle \mu | \mathbf{p} | \nu \rangle = \frac{m}{\hbar} \nabla_{\mathbf{k}} \langle \mu | H_{\mathbf{k} \cdot \mathbf{p}} | \nu \rangle. \quad (6a)$$

It should be stressed that this holds only for  $\mathbf{k}$ -independent basis functions  $|\mu\rangle$ , such as those in  $\mathbf{u}_{\text{at}}$  (3). The discussion above implies that the strain can be included simply through

$$\langle \mu | \mathbf{p}_\varepsilon | \nu \rangle = \frac{m}{\hbar} \nabla_{\mathbf{k}_\varepsilon} \langle \mu | H_{\mathbf{k} \cdot \mathbf{p}}(\mathbf{k}_\varepsilon, \varepsilon) | \nu \rangle. \quad (6b)$$

From  $\mathbf{H}_1$  (4d) and  $\mathbf{H}_2$  (4e) we obtain for the  $x$  component within the basis (3) the representation

$$\mathbf{p}_x(\mathbf{k}, \varepsilon) = \begin{bmatrix} \mathbf{p4}_x(\mathbf{k}_\varepsilon) & 0 \\ 0 & \mathbf{p4}_x(\mathbf{k}_\varepsilon) \end{bmatrix}, \quad (7)$$

with

$$\mathbf{p4}_x(\mathbf{k}_\varepsilon) = \frac{m}{\hbar} \begin{bmatrix} 0 & iP & 0 & 0 \\ -iP & 0 & 0 & 0 \\ 0 & 0 & 0 & 0 \\ 0 & 0 & 0 & 0 \end{bmatrix} + \frac{m}{\hbar} \begin{bmatrix} 2Ak_{x\varepsilon} & 0 & 0 & 0 \\ 0 & 2Lk_{x\varepsilon} & Nk_{y\varepsilon} & Nk_{z\varepsilon} \\ 0 & Nk_{y\varepsilon} & 2Mk_{x\varepsilon} & 0 \\ 0 & Nk_{z\varepsilon} & 0 & 2Mk_{x\varepsilon} \end{bmatrix} \quad (7')$$

and similar expressions for the other components,  $\mathbf{p}_y$  and  $\mathbf{p}_z$ .

#### D. Comparison with other approaches

In a reexamination of the signs of the imaginary elements in  $\mathbf{H}_\Delta$  we have obtained the same ones as Jones and O'Reilly,<sup>17</sup> while other authors have written down opposite ones (e.g., Refs. 6 and 9). These signs become important when the phases of the wave functions are significant.

Since both the first-order and the second-order  $\mathbf{k}$  terms are transformed in the same manner, all terms of the Hamiltonian (4) exhibit the symmetry of the strained crystal and the von Neumann principle is obeyed. However, in the second-order  $\mathbf{k}$  terms (4e), the factor  $(1 - \varepsilon)$  creates terms of the order  $\varepsilon^2$  not usually included in the transformation of the kinetic and potential energy operators. Probably this is the reason that most authors omit the factor  $(1 - \varepsilon) : (1 - \varepsilon)$  in the  $k^2$  terms. But it is evident

that this omission destroys the symmetry of the Hamiltonian matrix with strain. We believe, however, that consistency in symmetry is superior to consistency resting on the order of approximation.

As an example, we consider the momentum operator. Obviously, the representation (7) exhibits the same symmetry as the Hamiltonian (4) and, thus, obeys von Neumann's principle. As shown above, its derivation seems to be natural, while any other variant either violates the symmetry principle, or introduces artificial terms or *ad hoc* assumptions.

Many authors keep only the  $\mathbf{k}$ -independent "P terms" [first matrix in  $\mathbf{p4}_x$ , Eq. (7)] and neglect the free-electron contributions to the momentum operator and others from the interaction with the remote states [second matrix in  $\mathbf{p4}_x$ , Eq. (7)]. These contributions reflect the intimate connection between second-order perturbation theory for the Hamiltonian and first-order perturbation theory for the basis functions. All these terms vanish for  $k = 0$ , but may become significant for the Fermi momentum  $k$

values in highly doped or pumped samples, as will be demonstrated in a numerical example below.

Any consistent definition of the momentum operator in different representations should be compatible with the following general relation, which is exact within the energy representation:<sup>14</sup>

$$\langle \mu \mathbf{k} | \mathbf{p} | \mu \mathbf{k} \rangle = \frac{m}{\hbar} \nabla_{\mathbf{k}} E_{\mu}(\mathbf{k}) \quad (8a)$$

[ $|\mu \mathbf{k}\rangle$  denotes the band state with energy  $E_{\mu}(\mathbf{k})$ ]. According to the foregoing discussion, Eq. (8a) generalizes under strain to

$$\langle \mu \epsilon \mathbf{k}_{\epsilon} | \mathbf{p}_{\epsilon} | \mu \epsilon \mathbf{k}_{\epsilon} \rangle = \frac{m}{\hbar} \nabla_{\mathbf{k}_{\epsilon}} E_{\mu \epsilon}(\mathbf{k}_{\epsilon}, \epsilon). \quad (8b)$$

Equations (8) parallel the relation  $\mathbf{v}_g = \partial \omega / \partial \mathbf{k}$ ; i.e., the mean velocity of an electron or hole in state  $|\mu \epsilon \mathbf{k}_{\epsilon}\rangle$  equals the group velocity of the corresponding wave packet.

The omission of the free particle and remote states contributions ( $k^2$  terms) in the momentum matrix leads to the result that Eqs. (8) are no longer fulfilled (but at  $k=0$ , of course). The proof is straightforward for a two-band model. For the eight-band model, Eq. (8b) has been verified numerically.<sup>18</sup> Consequently, a consistent treatment of the  $\mathbf{k} \cdot \mathbf{p}$  momentum operator requires not only to keep the  $k^2$  terms, but to perform additionally the Pikus-Bir transformation in the Hamiltonian and in the momentum matrix for these terms.

### III. NUMERICAL RESULTS AND DISCUSSION

We have computed numerically the band structure, the wave functions, and the oscillator strengths from the  $8 \times 8$  Hamiltonian (4) for biaxially strained bulklike  $\text{In}_{0.71}\text{Ga}_{0.29}\text{As}_{0.62}\text{P}_{0.38}$  being closely lattice matched to InP. It is an interesting material for optoelectronic applications (it lases at a wavelength of  $\lambda=1.3 \mu\text{m}$ ), but has not been greatly investigated by means of the eight-band model. The material parameters are calculated from the quadratic interpolation formula<sup>19</sup> and the values of the binary compounds as listed by Adachi<sup>20</sup> and Krijn,<sup>21</sup> respectively; see Table I. It should be noted that the accurate measurement of the hole band masses in these

quaternary compounds is still an unsolved problem, though for the qualitative results to be stressed in this section, this plays a minor role.

The biaxial deformation tensor reads

$$\epsilon = \begin{pmatrix} \epsilon & 0 & 0 \\ 0 & \epsilon & 0 \\ 0 & 0 & C_p \epsilon \end{pmatrix}, \quad C_p \equiv -2 \frac{C_{12}}{C_{11}}. \quad (9)$$

Thus,  $\epsilon > 0$  ( $\epsilon < 0$ ) means tension (compression) in the  $xy$  plane.

#### A. Energy bands

The conduction band ( $C$ ) and the split-off band ( $SO$ ) behave smoothly under strain. The band edges without strain ( $k=0, \epsilon=0$ ),  $E_C(0,0)=E_g$ , and  $E_{SO}(0,0)=-\Delta$  are shifted by  $\Delta E_C(0,\epsilon)=a_c(2+C_p)\epsilon$  and, in the linear regime ( $|\epsilon| < 1\%$ ), by  $\Delta E_{SO}(0,\epsilon)=(1/3)(l_{\epsilon}+2m_{\epsilon})(2+C_p)\epsilon$ , respectively. The effective masses,  $m_C$  and  $m_{SO}$ , change only little. The strain-induced coupling between  $SO$  and  $LH$  affects the  $SO$  band only for rather high strain values (say,  $|\epsilon| > 1\%$ ). Therefore, we concentrate on the  $\Gamma_8$  valence-band complex, the heavy- ( $HH$ ) and light-hole states ( $LH$ ). Figure 1 illustrates characteristic features of the band structure for different strains. The splitting of the band edges and the drastic changes of the effective masses for  $\mathbf{k}$  directions not parallel to the  $z$  axis are typical for this class of semiconductors.

For tensile strain [Fig. 1(a)], the  $LH$  states are  $HH$ -like in all  $\mathbf{k}$  directions, except  $\mathbf{k}||z$ , and vice versa. This "exchange of effective masses" between  $HH$  and  $LH$  reflects a repulsive interaction between both bands, which is due to the symmetry reduction. For compressive strain [Fig. 1(c)], the  $HH$  effective mass in the  $x$  direction is smaller than that of the  $LH$ . But the repulsive interaction just mentioned causes an anticrossing of both bands. We will return to this interaction when discussing the symmetry of the  $HH$  and  $LH$  states.

Therefore, under stress, the notions  $HH$  and  $LH$  as used in Fig. 1 lose their original meaning, since the effective masses of both bands strongly depend on the  $\mathbf{k}$  direction. For biaxial stress with the stress axis in the  $z$  direction [cf. Eq. (9)], the conventional band curvature is

TABLE I. Material parameters for unstrained  $1.3\text{-}\mu\text{m-In}_x\text{Ga}_{1-x}\text{As}_y\text{P}_{1-y}$  on InP.

Parameter	Notion	Value	Unit
Fundamental gap	$E_g$	0.96 <sup>a</sup>	eV
Conduction-band mass	$m_c$	0.055	$m_0$
Heavy-hole mass in [100] direction	$m_{HH}$	0.692	$m_0$
Heavy-hole mass in [111] direction	$m_{HH111}$	1.0	$m_0$
Light-hole mass in [100] direction	$m_{LH}$	0.065	$m_0$
Spin-orbit split-off energy	$\Delta$	0.267	eV
Deformation potential of conduction band	$a_c$	-5.672	eV
Deformation potential of valence band	$a_v$	+1.179	eV
Shear deformation potential	$b$	-1.695	eV
Elastic constant	$C_{11}$	$1.0 \times 10^{12}$	$\text{kg m}^{-2}$
Elastic constant	$C_{12}$	$5.2 \times 10^{11}$	$\text{kg m}^{-2}$
Lattice constant, nominally unstrained	$a_0$	0.5867	nm

<sup>a</sup>Reference 26.

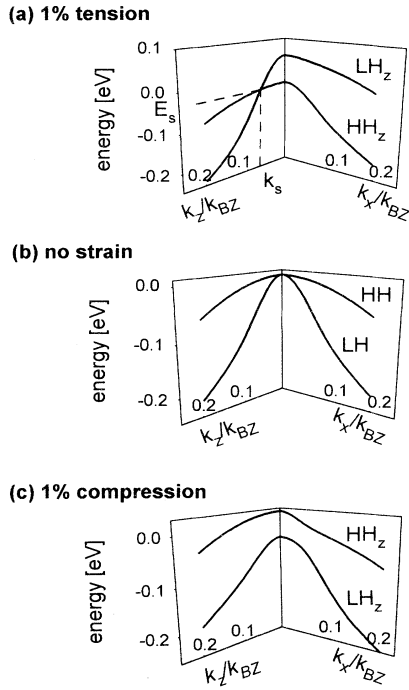


FIG. 1. Heavy- ( $\text{HH}_z$ ) and light- ( $\text{LH}_z$ ) hole bands in strained and unstrained bulklike  $1.3\text{-}\mu\text{m-In}_x\text{Ga}_{1-x}\text{As}_y\text{P}_{1-y}$  on InP; conventional band labeling (see text). (a) tensile strain:  $\epsilon=1\%$ ; both bands cross at  $\mathbf{k}=\mathbf{k}_s=(0,0,\pm k_s)$ ,  $E_{\text{HH}_z}(\mathbf{k}_s)=E_{\text{LH}_z}(\mathbf{k}_s)=E_s$ ; (b) no strain:  $\epsilon=0$ ; (c) compressive strain:  $\epsilon=-1\%$ . The cases  $\mathbf{k}\parallel[010]$ ,  $\mathbf{k}\parallel[110]$ , etc. are similar to  $\mathbf{k}\parallel\mathbf{x}$ . Crystal momentum,  $k$ , in units of  $k_{\text{BZ}}=\pi/a_0$  ( $a_0$  is the lattice constant of unstrained crystal). Such high strain values have been chosen in order to depict clearly the qualitative features.

preserved only in the  $z$  direction. In order to indicate this change, we will label these states  $\text{HH}_z$  and  $\text{LH}_z$ , respectively. Actually, these band energies are not analytical functions of crystal momentum and strain at  $\epsilon=0$  (cf. Refs. 4, 11, and 12). This singularity is also found in the strain dependence of the effective masses.<sup>19</sup>

In principle, there are two possibilities to label the  $\Gamma_8$  valence-band complex. (i) According to their symmetry at the  $\Gamma$  point,  $k=0$ . This is the most usual form and will be referred to as *conventional ordering*. It has been used in Fig. 1. It involves that the  $\text{HH}_z$  energy,  $E_{\text{HH}}$ , decreases with increasing  $\epsilon$  (tensile strain in the  $xy$  plane), while the  $\text{LH}_z$  energy,  $E_{\text{LH}}$ , increases. For  $\mathbf{k}\parallel\mathbf{z}$ , the  $\text{HH}_z$  band separates. For  $\mathbf{k}$  not parallel to  $\mathbf{z}$ , the bands are deliberately assigned as follows:  $E_{\text{HH}} < E_{\text{LH}}$  for  $\epsilon > 0$  and  $E_{\text{HH}} \geq E_{\text{LH}}$  for  $\epsilon \leq 0$ , respectively. (ii) Strict energetic level ordering. This will be referred to as *energetic ordering*. The energetically higher/lower states will be grouped into the upper/lower valence band (UVB/LVB):  $E_{\text{UV}} \geq E_{\text{LV}}$  for  $\epsilon > 0$  and for  $\epsilon \leq 0$ . Both schemes have their advantages and disadvantages.

For the isoenergy surfaces, the energetic ordering is appropriate. For no and compressive strain and sufficiently small  $k$  values, the isoenergy surfaces are warped ellipsoids, cf. Ref. 10. For tensile strain, however, the UVB and LVB touch in the  $\text{HH}_z$ - $\text{LH}_z$  crossing points

$\mathbf{k}_s(\epsilon)=(0,0,\pm k_s(\epsilon))$ ; see Fig. 1(a). Figure 2 displays the UVB and LVB isoenergetic surfaces for energies near and equal to the energy  $E_s=E_{\text{UV}}[\mathbf{k}_s(\epsilon)]=E_{\text{LV}}[\mathbf{k}_s(\epsilon)]$ . Note the similarity to the indicatrix of a birefringent biaxial crystals, cf. Ref. 15.

## B. Symmetry of the wave functions and character of the states

A more detailed analysis of the band dispersions depicted in Fig. 1 requires calculation of the symmetry of wave functions involved. In particular, a band anticrossing is accompanied with a change of the symmetry of the involved states. The symmetry of the band wave functions is determined by the contributions (portions) of the atomiclike basis functions (3). For  $z$  the quantization axis, the wave functions at  $k=\epsilon=0$  can be written in a comprehensive form as (cf., e.g., Ref. 9)

$$\begin{pmatrix} C_1 \\ \text{HH}_1 \\ \text{LH}_1 \\ \text{SO}_1 \\ C_2 \\ \text{HH}_2 \\ \text{LH}_2 \\ \text{SO}_2 \end{pmatrix}^{(z)} = \begin{pmatrix} iS \downarrow \\ \frac{X+iY}{\sqrt{2}} \uparrow \\ \frac{X-iY}{\sqrt{6}} \uparrow + \frac{2Z}{\sqrt{6}} \downarrow \\ \frac{X-iY}{\sqrt{3}} \uparrow - \frac{Z}{\sqrt{3}} \downarrow \\ iS \uparrow \\ \frac{X-iY}{\sqrt{2}} \downarrow \\ \frac{X+iY}{\sqrt{6}} \downarrow - \frac{2Z}{\sqrt{6}} \uparrow \\ \frac{X+iY}{\sqrt{3}} \downarrow + \frac{Z}{\sqrt{3}} \uparrow \end{pmatrix}. \quad (10a)$$

Characteristic features are the isotropy of  $C$  and  $\text{SO}$  states and lack of a  $z$  component in  $\text{HH}$  states. The  $C$  and  $\text{SO}$  wave functions are only less affected by the strain (9); therefore, their  $\mathbf{k}$  dependence is very similar to the strain-free case. For them, one obtains essentially the same results as Kane<sup>8</sup> did for InSb. Consequently, we will concentrate on the strain and  $\mathbf{k}$  dependence of the  $\Gamma_8$  group states. For the understanding of the symmetry of these states, it is essential to note that the eigenfunctions for  $\mathbf{x}$  being the quantization axis,

$$\begin{pmatrix} C_1 \\ \text{HH}_1 \\ \text{LH}_1 \\ \text{SO}_1 \\ C_2 \\ \text{HH}_2 \\ \text{LH}_2 \\ \text{SO}_2 \end{pmatrix}^{(x)} = \begin{pmatrix} iS \downarrow \\ \frac{-iY}{\sqrt{2}} \uparrow + \frac{Z}{\sqrt{2}} \downarrow \\ \frac{2X+iY}{\sqrt{6}} \uparrow + \frac{Z}{\sqrt{6}} \downarrow \\ \frac{X-iY}{\sqrt{3}} \uparrow - \frac{Z}{\sqrt{3}} \downarrow \\ iS \uparrow \\ \frac{X-iY}{\sqrt{2}} \downarrow + \frac{Z}{\sqrt{2}} \uparrow \\ \frac{2X-iY}{\sqrt{6}} \downarrow - \frac{Z}{\sqrt{6}} \uparrow \\ \frac{X+iY}{\sqrt{3}} \downarrow + \frac{Z}{\sqrt{3}} \uparrow \end{pmatrix}. \quad (10b)$$

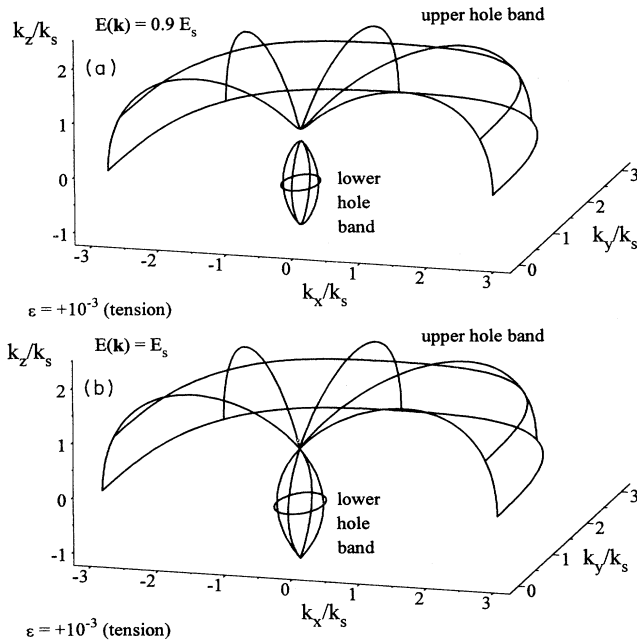


FIG. 2. Isoenergetic surfaces of the upper (UVB) and lower (LVB) valence bands in  $\mathbf{k}$  space:  $E_{UVB}(\mathbf{k}) = E_{LVB}(\mathbf{k}) = E = \text{const.}$  Tensile strain:  $\epsilon = +0.1\%$ . (a)  $E = 0.9E_s$ ; (b)  $E = E_s$ .  $k$  values in units of  $k_s$ .  $E_s$  is the energy of the  $\text{HH}_z$ - $\text{LH}_z$  crossing point  $\mathbf{k}_s = (0, 0, k_s)$ , cf. Fig. 1(a).

and for  $y$  being the quantization axis,

$$\begin{pmatrix} C_1 \\ \text{HH}_1 \\ \text{LH}_1 \\ \text{SO}_1 \\ C_2 \\ \text{HH}_2 \\ \text{LH}_2 \\ \text{SO}_2 \end{pmatrix}^{(y)} = \begin{pmatrix} iS \downarrow \\ \frac{X}{\sqrt{2}} \uparrow \frac{Z}{\sqrt{2}} \downarrow \\ \frac{X+2iY}{\sqrt{6}} \uparrow - \frac{Z}{\sqrt{6}} \downarrow \\ \frac{-X+iY}{\sqrt{3}} \uparrow + \frac{Z}{\sqrt{3}} \downarrow \\ iS \uparrow \\ \frac{X}{\sqrt{2}} \downarrow \frac{Z}{\sqrt{2}} \uparrow \\ \frac{-X+2iY}{\sqrt{6}} \downarrow + \frac{Z}{\sqrt{6}} \uparrow \\ \frac{X+iY}{\sqrt{3}} \downarrow - \frac{Z}{\sqrt{3}} \uparrow \end{pmatrix}, \quad (10c)$$

are *also* eigenfunctions of the (unstrained) Hamiltonian,  $\mathbf{H}_0 + \mathbf{H}_\Delta$ , and of the angular momentum. The functions (10a)–(10c) are the limiting cases of the wave functions for  $k \rightarrow 0$  and  $\mathbf{k} \parallel \mathbf{z}$ ,  $\mathbf{k} \parallel \mathbf{x}$ , and  $\mathbf{k} \parallel \mathbf{y}$ , respectively. Due to the degeneracy of HH and LH at  $k = 0$ , there is no unique limit for  $k \rightarrow 0$ , but a dependence on the direction of  $\mathbf{k}$ .

In the unstrained crystal, the  $\mathbf{k} \cdot \mathbf{p}$  interaction polarizes the states along the direction of  $\mathbf{k}$ .<sup>22</sup> Within the basis  $X$ ,  $Y$ , and  $Z$  for the valence bands [see Eq. (3)], the HH wave function has no component in the direction of  $\mathbf{k}$ . As  $\mathbf{k}$  rotates, the composition of the valence-band states changes accordingly. Note that this is even necessary for

the bands to be optically isotropic in the cubic crystal. For small  $k$  values, the composition of the LH wave functions is determined by the spin-orbit interaction. For large  $k$  values, it becomes, aside from phase factors, equal to that of the HH wave functions. Accordingly, both energy bands become parallel, cf. Fig. 1(b).

In a strained crystal, this polarization by the direction of quasiparticle motion may compete with the preference direction imposed by the strain. The interplay of strain, spin-orbit interaction, and  $\mathbf{k} \cdot \mathbf{p}$  interaction in the symmetry of the HH and LH wave functions is depicted in Fig. 3. For small  $k$  values, the composition is determined by the strain. The  $z$  axis exhibits fourfold rotation symmetry, while the  $x$  and  $y$  axes exhibit only twofold. This makes the  $z$  axis the axis of quantization. The wave functions are given by Eq. (10a). In the unstrained case, as here  $\mathbf{k} \parallel \mathbf{x}$ ,  $\mathbf{x}$  is the axis of quantization, and the wave functions are given by Eq. (10b).

As the  $k_x$  value increases, the  $X$  component decreases in Figs. 3(a), 3(d), and 3(f), and the states become HH-

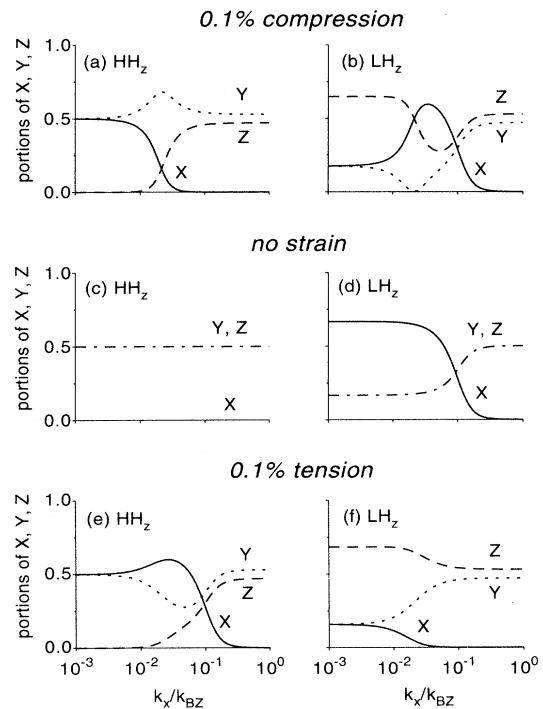


FIG. 3. Relative portions of the basis functions  $X$ ,  $Y$ , and  $Z$  in the heavy- ( $\text{HH}_z$ ) and light-hole ( $\text{LH}_z$ ) wave functions  $\mathbf{u}_{\text{HH}}(k_x, \epsilon)$  and  $\mathbf{u}_{\text{LH}}(k_x, \epsilon)$  (conventional band labeling, cf. Fig. 1).  $k_y = k_z = 0$ . The wave functions  $\mathbf{u}_{\text{HH}}(0, 0)$  and  $\mathbf{u}_{\text{LH}}(0, 0)$  have been deliberately set to guarantee continuity. (a), (b)  $\epsilon = -10^{-3}$  (compression in the  $xy$  plane), heavy-hole/light-hole band. (c), (d)  $\epsilon = 0$  (no strain), heavy-hole/light-hole band. (e), (f)  $\epsilon = +10^{-3}$  (tension in the  $xy$  plane), heavy-hole/light-hole band. Note that the  $S$  portion in the  $\text{HH}_z$  and  $\text{LH}_z$  wave functions remains very small for all  $k_x$  and  $\epsilon$  values, even for the medium  $k_x$  range. Thus, the exchange of  $s$ - and  $p$ -like basis states between the conduction- and the valence-band states caused by the  $\mathbf{k} \cdot \mathbf{p}$  interaction is carried almost completely by the SO band alone.

like. In contrast, the states in Figs. 3(b) and 3(e) become LH-like with respect to the axis of quantization  $\mathbf{x}$  and the spin-orbit interaction being the dominant interaction. In the case of tensile strain and medium  $k$  values,  $\mathbf{k}$  not parallel to  $\mathbf{z}$ , the standard labeling is misleading [ $k_x = 10^{-2} - 10^{-1} k_{\text{BZ}}$  in Figs. 3(e) and 3(f)].

For large  $k$  values, the  $\mathbf{k} \cdot \mathbf{p}$  interaction dominates. Besides the factor  $(1 - \epsilon)$  introduced by the Pikus-Bir transformation, it is isotropic. Correspondingly, in all cases shown in Fig. 3, the symmetry is HH-like. As the small differences between the  $Y$  and the  $Z$  portions are caused mainly by terms of first order in the strain, the wave functions in Fig. 3(e) [3(f)] are LH-(HH)-like, in contrast to the standard labeling.

Consequently, for small  $k$  values, the standard labeling is appropriate, while for larger  $k$  values,  $\mathbf{k}$  not parallel to  $\mathbf{z}$ , the energetic labeling is. A similar behavior has been found for biaxially strained semimagnetic semiconductors in an external magnetic field  $\mathbf{B} \parallel \mathbf{x}$ .<sup>23</sup>

The symmetry of the states determines the optical selection rules. Within the eight-band model, the oscillator strength for interband transitions and an electromagnetic field being linearly polarized in, say, the  $x$  direction is determined by the  $S$  component of the wave function of one band state and the  $X$  component of the other one. Thus, we obtain dichroism for optical transitions near the band gaps and isotropy for larger photon energies.

### C. Momentum matrix and oscillator strengths

The “irregular” behavior of the symmetry of the heavy- and light-hole wave functions in dependence of  $\epsilon$  and  $\mathbf{k}$  should be reflected in the dispersion of the oscillator strengths. In order to quantify the importance of a consistent treatment of the momentum operator, we have calculated numerically the interband oscillator strengths,

$$f_{\epsilon\mu\nu}^{\alpha}(\mathbf{k}_{\epsilon}, \epsilon) = \frac{2}{m_0} \sum_{\sigma, \rho=1}^2 \frac{|\langle \mu\sigma\epsilon\mathbf{k}_{\epsilon} | \mathbf{p}_{\epsilon\alpha} | \nu\rho\epsilon\mathbf{k}_{\epsilon} \rangle|^2}{E_{\mu\epsilon}(\mathbf{k}_{\epsilon}, \epsilon) - E_{\nu\epsilon}(\mathbf{k}_{\epsilon}, \epsilon)} \quad (11)$$

( $\mu = C$ ;  $\nu = \text{HH, LH}$ ;  $\rho, \sigma = 1, 2$ , the Kramers degenerate subband indices). A projection operator technique has been used, which circumvents the evaluation of the wave functions (see the Appendix). In Fig. 4, some results obtained by means of the exact formula (6b) are compared with those of two common approximations for the momentum matrix. In the first one, the  $\mathbf{k}$ -dependent terms [second matrix in  $\mathbf{p}_4^x$ , Eq. (7)] are neglected. The second one is the effective-mass approximation,

$$\mathbf{p}_{\epsilon\mu\nu}(\mathbf{k}_{\epsilon}, \epsilon) = \mathbf{p}_{\epsilon\mu\nu}(\mathbf{0}, \epsilon) \frac{E_{\mu\epsilon}(\mathbf{0}, \epsilon) - E_{\nu\epsilon}(\mathbf{0}, \epsilon)}{E_{\mu\epsilon}(\mathbf{k}_{\epsilon}, \epsilon) - E_{\nu\epsilon}(\mathbf{k}_{\epsilon}, \epsilon)}, \quad \mu \neq \nu \quad (12)$$

for allowed transitions.

Obviously, the deviations of both approximations from the exact results are small in unstrained materials, while the effective-mass approximation (12) fails principally in strained crystals. The reason for that is the following. Since the momentum operator has a defined parity (odd), the oscillator strength becomes sensitive to detect the symmetry of the involved states. The band mixing effects discussed above result in nonmonotonous compositions of

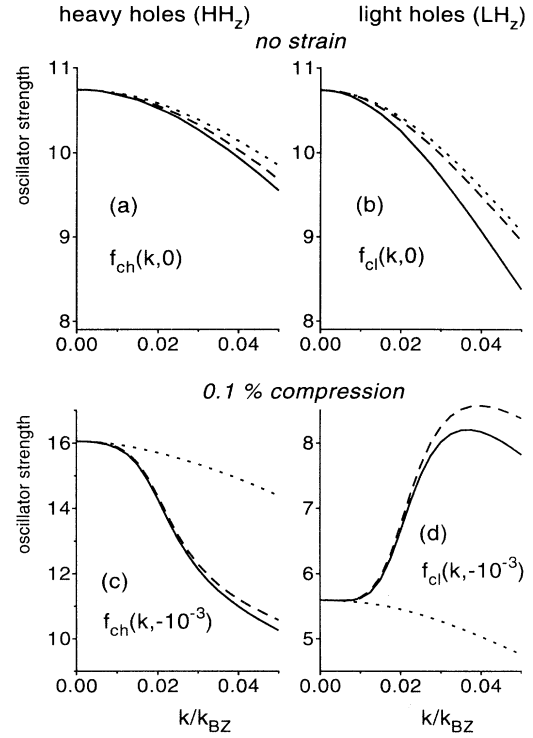


FIG. 4. Oscillator strengths,  $f(k, \epsilon)$ , of transitions C-HH<sub>z</sub> and C-LH<sub>z</sub> as functions of  $k$  ( $k$  in units of  $k_{\text{BZ}} = \pi/a_0$ ). (a) C-HH<sub>z</sub>,  $\epsilon = 0$ ; (b) C-LH<sub>z</sub>,  $\epsilon = 0$ ; (c) C-HH<sub>z</sub>,  $\epsilon = -10^{-3}$  (compression); (d) C-LH<sub>z</sub>,  $\epsilon = -10^{-3}$  (compression). Full lines: consistent definition of the momentum matrix elements and numerically exact diagonalization of the eight-band Hamiltonian; dotted lines: effective-mass approximation, Eq. (12); dashed lines: omission of the  $k^2$  terms in the momentum matrix, cf. Eq. (7'). The oscillator strengths shown are values averaged over the  $k$ -space directions  $\mathbf{x}$ ,  $\mathbf{y}$ , and  $\mathbf{z}$  as  $f_{\epsilon\mu\nu}^{\alpha}(\mathbf{k}_{\epsilon}, \epsilon) = [f_{\epsilon\mu\nu}^{\alpha}(k_x, \epsilon) + f_{\epsilon\mu\nu}^{\alpha}(k_y, \epsilon) + f_{\epsilon\mu\nu}^{\alpha}(k_z, \epsilon)]/3$ . This neglects the angular dispersion of the energy bands, but the purpose here is to demonstrate the qualitative failure of the effective-mass approximation for strained materials.

the hole wave functions and, therefore, in nonmonotonous dispersion of the oscillator strength. This behavior cannot be reproduced by Eq. (12), since the gaps are monotonous functions of  $\epsilon$  and  $\mathbf{k}$ . Consequently, extrapolations from the  $\Gamma$  point to the case  $k > 0$  are by no means a valid approximation, especially in strained crystals.

## IV. SUMMARY AND CONCLUSIONS

We have reconsidered the  $\mathbf{k} \cdot \mathbf{p}$  theory for homogeneously strained semiconductors with particular attention to the second-order  $\mathbf{k}$  terms and the momentum operator. Our main results are the following. (i) The second-order terms have to be multiplied with  $(1 - \epsilon):(1 - \epsilon)$ , in order to obey basic requirements of symmetry, although this procedure introduces contributions which are of second order in the strain  $\epsilon$ . (ii) The second-order  $\mathbf{k}$  terms are to be included in the framework of a consistent treatment of the momentum operator. (iii) There is a heavy-hole and



light-hole band mixing and anticrossing, except along some higher-symmetric directions. Consequently, extrapolations of  $k$ -dependent parameters from the  $\Gamma$  point to values of  $k > 0$  are not straightforward. Moreover, the notions of light-hole band and heavy-hole band can become misleading for  $k > 0$  when considering the symmetry of these states, since the latter changes dramatically as a consequence of state mixing. This is important to recognize for the interpretation of the optical properties of strained materials.<sup>24</sup>

Numerical results for the band structure have shown bulklike  $1.3\text{-}\mu\text{m-In}_x\text{Ga}_{1-x}\text{As}_y\text{P}_{1-y}$  nearly lattice matched to InP as a representative of this class of semiconductors. Hence, our results for the momentum operator and oscillator strengths should apply to other materials of this type as well. These are (i) that the neglect of the  $k^2$  terms can result in significant numerical deviations for practically relevant cases, and that (ii) the effective-mass approximation for the  $k$  dependence of the momentum matrix elements is applicable in special cases only. In unstrained materials, the effective-mass approximation produces, in general, a too weak  $k$  dependence of the oscillator strengths; while in strained material, it is not able to reproduce their nonmonotonous behavior at all. Consequently, a realistic model of momentum-related properties (e.g., optical properties, momentum relaxation) requires (i) a consistent definition of the momentum operator within the representation considered, such as Eqs. (6) and (7) and (ii) the calculation of its energy representation by means of an exact method (cf. also Ref. 4).

Thus, we have presented band structure, wave function, and oscillator strength calculations for  $1.3\text{-}\mu\text{m-In}_x\text{Ga}_{1-x}\text{As}_y\text{P}_{1-y}$  on InP using an eight-band  $k\cdot p$  model and accounting for the von Neumann symmetry principle and consistency of the momentum operator. These results can be useful also as asymptotic values for investigations on quantum wells of varying thickness, and the formulas used may serve as a starting point for computing the polarization and strain dependence of optical properties of this material.<sup>25</sup>

#### ACKNOWLEDGMENTS

The authors thank Professor T. Elsässer for helpful discussions and a critical reading of the manuscript. This work was supported by the Deutsche Forschungsgemeinschaft (DFG).

#### APPENDIX: PROJECTION OPERATOR METHOD FOR CALCULATING THE OSCILLATOR STRENGTH WITHOUT WAVE FUNCTION

The projection operator

$$P_{\nu\mathbf{k}}(\mathbf{r}, \mathbf{r}') = \sum_{\rho} \psi_{\nu\rho\mathbf{k}}(\mathbf{r}) \psi_{\nu\rho\mathbf{k}}(\mathbf{r}')^* \quad (\text{A1})$$

projects on the subspace of the eigenstates  $\psi_{\nu\rho\mathbf{k}}(\mathbf{r})$  of the Hamiltonian  $H$  to the band  $\nu$  and crystal momentum  $\mathbf{k}$  ( $\rho$  degeneracy index):

$$H(\mathbf{r}, \mathbf{r}') \psi_{\nu\rho\mathbf{k}}(\mathbf{r}') = \sum_{\mu\sigma} \psi_{\mu\sigma\mathbf{k}}(\mathbf{r}) \int \int \int \psi_{\mu\sigma\mathbf{k}}(\mathbf{r}')^* \left[ -\frac{\hbar^2}{2m} \nabla_{\mathbf{r}'} + V(\mathbf{r}') \right] \psi_{\nu\rho\mathbf{k}}(\mathbf{r}') d\mathbf{r}' = E_{\nu\mathbf{k}} \psi_{\nu\rho\mathbf{k}}(\mathbf{r}), \quad (\text{A2})$$

$$P_{\nu\mathbf{k}}(\mathbf{r}, \mathbf{r}') \psi_{\mu\sigma\mathbf{k}}(\mathbf{r}) = \sum_{\rho} \psi_{\nu\rho\mathbf{k}}(\mathbf{r}) \int \int \int \psi_{\nu\rho\mathbf{k}}(\mathbf{r}')^* \psi_{\mu\sigma\mathbf{k}}(\mathbf{r}') d\mathbf{r}' = \delta_{\mu\nu} \psi_{\nu\sigma\mathbf{k}}(\mathbf{r}). \quad (\text{A3})$$

The optical matrix elements entering the oscillator strength can be expressed as follows:

$$|\langle \mu\sigma\mathbf{k} | \mathbf{p} | \nu\rho\mathbf{k} \rangle|^2 = \sum_{\rho\sigma} \int \int \int \psi_{\mu\sigma\mathbf{k}}(\mathbf{r})^* \mathbf{p} \psi_{\nu\rho\mathbf{k}}(\mathbf{r}) d\mathbf{r} \int \int \int \psi_{\nu\rho\mathbf{k}}(\mathbf{r}')^* \mathbf{p} \psi_{\mu\sigma\mathbf{k}}(\mathbf{r}') d\mathbf{r}' = \text{tr}(P_{\mu} \mathbf{p} P_{\nu} \mathbf{p}). \quad (\text{A4})$$

The trace opens alternative calculational options, since it is representation independent. The crucial point is that there is another formula for the projection operator,<sup>25</sup> which is independent of the eigenfunctions of the Hamiltonian,

$$P_{\nu\mathbf{k}} = \prod_{\mu \neq \nu} \frac{H - E_{\mu\mathbf{k}} \times 1}{E_{\nu\mathbf{k}} - E_{\mu\mathbf{k}}} \quad (\text{A5})$$

(1 is the unit operator). The proof is straightforward by using (A3) and (A2). Therefore,  $P_{\nu\mathbf{k}}$  and  $\mathbf{p}$  can be calculated most conveniently within the basis  $\mathbf{u}_{\text{at}}$ ; the eigenfunctions of  $H$  are not needed. The formalism even simplifies, when both  $\mathbf{H}$  and  $\mathbf{p}$  block diagonalize. Its ap-

plication to the calculation of higher-order transition probabilities entering the calculation of nonlinear optical properties is in progress.

Finally, we remark that from Eq. (A1), it follows immediately that

$$\sum_{\rho} |\langle u_{r\sigma} | \psi_{\nu\rho\mathbf{k}} \rangle|^2 = (P_{\nu\mathbf{k}})_{r\sigma, r\sigma}. \quad (\text{A6})$$

This means the portion of the basic state  $u_{r\sigma}$  in the eigenstate  $\psi_{\nu\rho\mathbf{k}}$  equals the corresponding diagonal matrix element of the projection operator onto the eigenstate  $\psi_{\nu\rho\mathbf{k}}$  in the representation of these basic states  $\{u_{r\sigma}\}$ .

- <sup>1</sup>J. M. Luttinger and W. Kohn, *Phys. Rev.* **97**, 869 (1955).
- <sup>2</sup>E. O. Kane, in *Handbook on Semiconductors*, edited by T. S. Moss (North-Holland, New York, 1982), Vol. 1, Chap. 4A.
- <sup>3</sup>H.-R. Trebin, U. Rössler, and R. Ranvaud, *Phys. Rev. B* **20**, 686 (1979).
- <sup>4</sup>G. L. Bir and G. E. Pikus, *Symmetry and Strain-Induced Effects in Semiconductors* (Wiley, New York, 1974).
- <sup>5</sup>T. B. Bahder, *Phys. Rev. B* **41**, 11 992 (1990).
- <sup>6</sup>G. E. Pikus and G. L. Bir, *Fiz. Tverd. Tela (Leningrad)* **1**, 1642 (1959) [*Sov. Phys. Solid State* **1**, 1502 (1960)].
- <sup>7</sup>A. P. Cracknell, *Angewandte Gruppentheorie* (Akademie-Verlag, Berlin, 1971), p. 49.
- <sup>8</sup>E. O. Kane, *J. Phys. Chem. Solids* **1**, 249 (1957).
- <sup>9</sup>S. L. Chuang, *Phys. Rev. B* **43**, 9649 (1991).
- <sup>10</sup>K. Suzuki and J. C. Hensel, *Phys. Rev. B* **9**, 4184 (1974).
- <sup>11</sup>J. C. Hensel and K. Suzuki, *Phys. Rev. B* **9**, 4219 (1974).
- <sup>12</sup>F. H. Pollak and M. Chandrasekhar, *Phys. Rev. B* **15**, 2127 (1977).
- <sup>13</sup>W. Brauer and H.-W. Streitwolf, *Theoretische Grundlagen der Halbleiterphysik* (Akademie-Verlag, Berlin, 1973), Appendix A.
- <sup>14</sup>M. Born and E. Wolf, *Principles of Optics*, 2nd ed. (Pergamon, New York, 1964), Fig. 14.9; A. Yariv and P. Yeh, *Optical Waves in Crystals* (Wiley, New York, 1984), Fig. 4.1.
- <sup>15</sup>W. Shockley, *Phys. Rev.* **78**, 173 (1950).
- <sup>16</sup>P. Enders, *Phys. Status Solidi B* **187**, 541 (1995).
- <sup>17</sup>G. Jones and E. P. O'Reilly, *IEEE J. Quantum Electron.* **29**, 1344 (1993).
- <sup>18</sup>P. Enders (unpublished).
- <sup>19</sup>*Semiconductors. Intrinsic Properties of Group IV Elements and III-V, II-IV, and I-VII Compounds*, Landolt-Börnstein: New Series, Group III, Vol. 22, Pt. a (Springer, Heidelberg, 1982).
- <sup>20</sup>S. Adachi, *J. Appl. Phys.* **53**, 8775 (1982).
- <sup>21</sup>M. P. C. Krijn, *Semicond. Sci. Technol.* **6**, 27 (1991).
- <sup>22</sup>I. M. Tsidil'kovskii', *Band Structure of Semiconductors* (Nauka, Moscow, 1978), p. 74 (in Russian).
- <sup>23</sup>C. Santos, D. Suisky, P. Enders, F. Neugebauer, M. Hartmann, J. Röseler, and W. Heimbrod (unpublished).
- <sup>24</sup>P. Enders, A. Bärwolff, R. Müller, and T. Elsässer (unpublished).
- <sup>25</sup>O. Ziep (private communication).
- <sup>26</sup>G. P. Agrawal and N. K. Dutta, *Long-Wavelength Semiconductor Lasers* (Van Nostrand, New York, 1986).